Design and Synthesis of an Orally Bioavailable and Selective Peptide Epoxyketone Proteasome Inhibitor (PR-047)

Han-Jie Zhou,* Monette A. Aujay, Mark K. Bennett, Maya Dajee, Susan D. Demo, Ying Fang, Mark N. Ho, Jing Jiang, Christopher J. Kirk, Guy J. Laidig, Evan R. Lewis, Yan Lu, Tony Muchamuel, Francesco Parlati, Eileen Ring, Kevin D. Shenk, Jamie Shields, Peter J. Shwonek, Timothy Stanton, Congcong M. Sun, Catherine Sylvain, Tina M. Woo, and Jinfu Yang

Proteolix, Inc., 333 Allerton Avenue, South San Francisco, California 94080

Proteasome inhibition has been validated as a therapeutic modality in the treatment of multiple myeloma and Non-Hodgkin's lymphoma. Carfilzomib, an epoxyketone currently undergoing clinical trials in malignant diseases, is a highly selective inhibitor of the chymotrypsin-like (CT-L) activity of the proteasome. A chemistry effort was initiated to discover orally bioavailable analogues of carfilzomib, which would have potential for improved dosing flexibility and patient convenience over intravenously administered agents. The lead compound, 2-Me-5-thiazole-Ser(OMe)-Ser(OMe)-Phe-ketoepoxide (**58**) (PR-047), selectively inhibited CT-L activity of both the constitutive proteasome (β5) and immunoproteasome (LMP7) and demonstrated an absolute bioavailability of up to 39% in rodents and dogs. It was well tolerated with repeated oral administration at doses resulting in >80% proteasome inhibition in most tissues and elicited an antitumor response equivalent to intravenously administered carfilzomib in multiple human tumor xenograft and mouse syngeneic models. The favorable pharmacologic profile supports its further development for the treatment of malignant diseases.

Introduction

The proteasome is a multicatalytic protease complex that is responsible for the ubiquitin-dependent turnover of cellular proteins.[1-3] Proteasome substrates include misfolded or mis-assembled proteins as well as short-lived components of signaling cascades that regulate cell proliferation and survival pathways. Inhibition of the proteasome leads to an accumulation of substrate proteins and results in cell death.[4] The proteasome consists of a 20S proteolytic core and two 19S regulatory caps that assemble with the core at either end to form a 26S complex.[5,6] Two distinct forms of the 26S proteasome, the constitutive proteasome and the immunoproteasome, have been identified. The majority of cell types express the constitutive form of the proteasome, while cells of the immune system express the immunoproteasome. Nonimmune cells can also express immunoproteasomes following exposure to inflammatory cytokines such as interferon γ (IFN-γ). The 20S core of the constitutive proteasome has three distinct catalytic activities: chymotrypsin-like (CT-L[a]), trypsin-like (T-L), and caspase-like (C-L), which are encoded by the β5, β2, and β1 subunits, respectively. Of these, the CT-L activity is thought to be the rate-limiting step of proteolysis in vitro and in vivo, while inhibition of multiple sites might be required to fully suppress proteasome-mediated protein turnover.[7,8] The immunoproteasome retains the structural subunits of the constitutive proteasome but incorporates the catalytic subunits LMP7, MECL1, and LMP2 in place of β5, β2, and β1, respectively.[9-12] Each proteasome active site utilizes the nucleophilic γ-hydroxyl group of an amino-terminal threonine (Thr) residue to initiate amide bond hydrolysis and activation of nucleophilic water by the α-amino group to hydrolyze the resulting ester.

Clinical validation of the proteasome as a therapeutic target in oncology has been provided by bortezomib **1** (Figure 1), a dipeptide boronic acid,[4,13] which is approved for the treatment of patients with multiple myeloma[14-17] and mantle cell lymphoma.[18,19] Although the clinical success of bortezomib is encouraging, a significant fraction of patients relapse or are refractory to treatment.[14-19] Additionally, dose-limiting toxicities (DLT), including a painful peripheral neuropathy and thrombocytopenia, have been reported.[16,20,21] It is unclear whether these toxicities can be attributed to off-target effects because bortezomib inhibits other enzymes such as serine proteases, albeit with lower potencies.[13,22,23] Recently, we reported the discovery of carfilzomib **2** (also called PR-171),[22,23] a structural analogue of the microbial natural product epoxomicin **3** that was initially identified for its antitumor activity and subsequently shown to be a potent inhibitor of the proteasome.[24-28] Carfilzomib selectively inhibits the CT-L activity of the 20S proteasome and displays equivalent potency against β5 and LMP7 with minimal cross reactivity to other protease classes. Preclinical studies and phase I clinical studies demonstrated that consecutive day dosing schedules with carfilzomib are both well tolerated and promote antitumor activity in hematologic malignancies, including patients previously treated with bortezomib.[22,23,29-33] Carfilzomib is currently being evaluated in phase I and phase II clinical trials in multiple myeloma, non-Hodgkin's lymphoma, and solid tumors.

Clinical responses to proteasome inhibitor therapy require frequent dosing (e.g., twice per week) and prolonged treatment. Both bortezomib and carfilzomib are administered intravenously (iv) on biweekly or more frequent dosing schedules with treatment that can extend for over 6 months.[23] Therefore, the development of orally bioavailable proteasome inhibitors that would allow for dosing flexibility and improve patient convenience is warranted. We describe here the results of systematic

---

* To whom correspondence should be addressed. Phone: (650)-504-8346. Fax: 650-872-1875. E-mail: hzhou@proteolix.com.

[a] Abbreviations: CT-L, chymotrypsin-like; T-L, trypsin-like; C-L, caspase-like; MDR, multidrug resistance transporters; SGF, simulated gastric fluids; SIF, simulated intestinal fluids; iv, intravenous administration; po, oral administration; PK, pharmacokinetics; PD, pharmacodynamics; DLT, dose limiting toxicities; MTD, maximum tolerated dose.
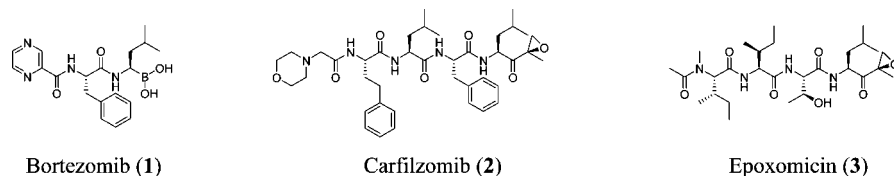
Figure 1. Structures of bortezomib, carfilzomib, and epoxomicin.

Table 1. Carfilzomib and Its Truncated Analogues

| compd	20S CT-L[a] IC_{50} (nM)	Molt-4 CT-L[a] IC_{50} (nM)	mice PO PD (% CT-L activity @ 40 mg/kg)			MES cell viability ± MDR[a] IC_{50} (nM)		stability (% parent @ 15 min)		liver microsome stability (R_e)	
			liver	blood	adrenal	MDR−	MDR+	SGF	SIF	mouse	human
2	5.7 ± 5.3 (139)	5.1 ± 2.7 (78)	109	77	83	18 ± 16 (46)	413 ± 237 (46)	∼15	<5	0.98	0.93
4	>1000	>1000	ND[b]	ND[b]	ND[b]	>1000	>1000	ND[b]	ND[b]	ND[b]	ND[b]
5	57 ± 42 (5)	45 ± 5 (4)	22	37	82	35 ± 10 (5)	308 ± 134 (5)	∼90	∼45	0.95	ND[b]

[a] All experiments to determine IC_{50} values were run with at least duplicates at each compound dilution; IC_{50} values were averaged when determined in two or more independent experiments; the individual IC_{50} values listed in parentheses ($n = 2$) or ± standard deviation denoted and n listed in parentheses ($n \geq 3$). [b] Not determined.

SAR studies to develop orally bioavailable epoxyketone-based proteasome inhibitors that maintain the potency, selectivity, and antitumor activity of carfilzomib.

Biological Assays

Inhibition of the CT-L activity was tested in cell free systems using purified human 20S proteasomes (Boston Biochem Inc., Cambridge, MA) and in cellular lysates prepared from Molt-4 (human leukemia) cells treated with inhibitors for 1 h. In both assays, 50% inhibitory concentrations (IC_{50}) were determined and comparison of the IC_{50} values using purified enzyme to intact cell exposure served as an assessment of the cell permeability of compounds.[22] Inactivation rates (k_{inact}/K_i) were determined for a subset of analogues using purified human 26S proteasome. Selectivity for proteasomal subunits was measured using an active site binding assay in lysates from inhibitor treated Molt-4 cells.[34] The sensitivity of compounds to multidrug resistance transporters (MDR) was evaluated by comparing cell viability on a pair of MES (uterine sarcoma) tumor cell lines: the parental line (MDR−) and a doxorubicin resistant subline known to express MDR (MDR+).[35] Compound stability was evaluated in simulated gastric and intestinal fluids (SGF and SIF), and the percentage of parent remaining was determined after 15 min of incubation. Metabolic stability was assessed in liver microsomes from mouse, rat, dog, and human, and the extraction ratio (R_e) was calculated based on half-life to facilitate cross-species comparisons.[36] Bioactivity was determined by pharmacodynamic (PD) measurements of residual CT-L activity in blood and tissues 1 h after oral (po) administration. Absolute bioavailability (F) was determined by pharmacokinetic (PK) assessment of areas under the plasma concentration versus time curves following iv and po administrations. Antitumor efficacy was assessed in immunocompromised mice bearing established human tumor xenografts and in normal mice bearing syngeneic tumor cells (see Supporting Information for more details on biological assays).

All compounds were tested against purified human 20S proteasomes and Molt-4 cells for inhibition of the proteasome CT-L activity. Compounds with IC_{50} less than 100 nM and solubility ≥1.0 mg/mL in a vehicle of 10% (v/v) EtOH and 10% (v/v) PS80 in citrate buffer (pH 3.5) were then orally administered to Balb/c mice (40, 20, 10, or 5 mg/kg) for initial assessment of bioavailability by blood and tissue PD (CT-L
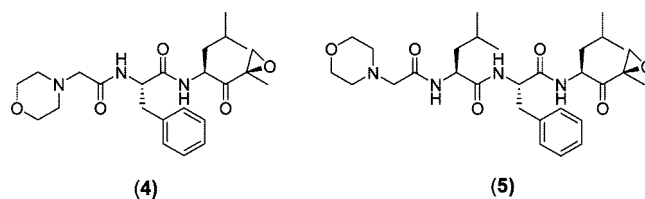

Figure 2. Structures of analogues **4** and **5**.

activity 1 h postdose). A subset of compounds was subsequently chosen for further evaluation in other aforementioned assays.

Results and Discussions

Carfilzomib Truncations. The starting point of our chemistry effort was carfilzomib, a tetrapeptide epoxyketone. Initially, we found that carfilzomib and its tetrapeptide derivatives failed to exhibit significant oral bioavailability as measured by inhibition of proteasome activity in blood or tissue following po administration to mice (Table 1). The instability of carfilzomib in SGF, SIF, and liver microsomes may each contribute to the lack of systemic exposure. These results are consistent with reports that di- and tripeptides can cross intestinal epithelial barriers, while tetrapeptides are generally not orally bioavailable.[37,38] To determine if shortening the peptide portion of carfilzomib would maintain potency and improve bioavailability, truncated di- and tripeptidyl analogues of carfilzomib were synthesized (Figure 2). The dipeptide epoxyketone **4** had weak potency against the CT-L activity of the 20S proteasome (>1000 nM). In contrast, the tripeptide epoxyketone **5** exhibited strong CT-L inhibitory activity, and importantly, induced proteasome inhibition in blood and liver following po administration to mice. Notably, compound **5** was stable in SGF and partially stable in SIF but unstable in liver microsomal assays across multiple species, perhaps contributing to the limited PD response in peripheral tissues such as adrenal after po dosing. On the basis of these initial results, further chemistry efforts were focused on tripeptide epoxyketone analogues.

N-Cap Screening on Tripeptide Ketoepoxide. The chemistry strategy began with screening N-terminus capping groups with a backbone of Leu-Phe-Leu-ketoepoxide. The N-caps included a variety of amides (primarily five- or six-membered aromatic or nonaromatic heterocycles) and ureas. Amides were synthesized by deprotection of a shared Boc-Leu-Phe-Leu-ketoepoxide intermediate and then coupling with various

Table 2. Screening N-Caps with Backbone of N-cap-Leu-Phe-Leu-Ketoepoxide
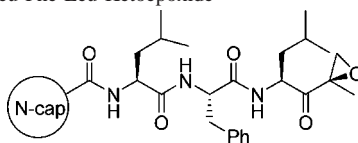
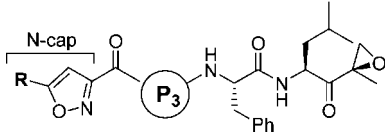| compd	N-cap	20S CT-L[a] IC$_{50}$ (nM)	Molt-4 CT-L[a] IC$_{50}$ (nM)	MES cell viability ± MDR[a] IC$_{50}$ (nM)	
				MDR−	MDR+
5	morpholine-CH$_2$	57 ± 42 (5)	45 ± 5 (4)	35 ± 10 (5)	308 ± 134 (5)
6	3-furan	34	116	54	125
7	2-thiophene	10 ± 5 (3)	40	34	120
8	5-oxazole	27	84	159	505
9	5-isoxazole	5.8 (3.7, 7.9)	65 ± 28 (3)	58 (56, 60)	82 (76, 88)
10	3-isoxazole	7.4 (3.7, 11)	50 ± 17 (3)	73 (55, 92)	123 (86, 159)
11	(5-Me)-3-isoxazole	1.8 ± 0.9 (5)	17 ± 12 (5)	28 (22, 34)	47 (32, 64)
12	(5-iPr)-3-Isoxazole	6.3	17 (15, 18)	63 (55, 71)	30 (24, 37)
13	(5-MeOCH$_2$)-3-isoxazole	1.2 (1.1, 1.3)	8.1 ± 4.3 (3)	23 (12, 35)	28 (26, 30)
14	3-pyrazole	36 ± 2 (3)	188 (135, 242)	109 (83, 134)	>1000
15	2-imidazole	107 (103, 110)	271 (222, 320)	136 (129, 142)	>1000
16	(N-Me)-3-Pyrazole	76 ± 32 (3)	290	137	205
17	(N-Me)-2-imidazole	122 (77, 167)	161	67	164
18	(5-Me)-3-pyrazole	38 (25, 51)	245	103	>1000
19	4-pyridine	20 (16, 23)	55	33	>1000
20	4-pyridazine	12 (9, 14)	50 (38, 63)	18 ± 2 (3)	>1000
21	2-pyrazine	752	>1000	>1000	>1000
22	2-(R)-Tetrahydrofuran	34	154	69	110
23	2-(S)-tetrahydrofuran	42 (31, 52)	180	130	159
24	(5-Me)-3-isoxazole-NH	13	47	182	>1000

[a] All experiments to determine IC$_{50}$ values were run with at least duplicates at each compound dilution; IC$_{50}$ values were averaged when determined in two or more independent experiments; the individual IC$_{50}$ values listed in parentheses ($n = 2$) or ± standard deviation denoted and n listed in parentheses ($n \geq 3$).

carboxylic acids under a coupling condition of HOBt/HBTU/DIEA. Ureas were prepared from the deprotected backbone and isocyanates. More than 100 N-cap variants were evaluated for potency against CT-L inhibition in purified human 20S proteasome and Molt-4 cells as well as MDR resistance in the paired MES-SA cell lines. Results from representative compounds are outlined in Table 2. Notably, five-membered heterocycles devoid of an NH group such as furan **6**, thiophene **7**, oxazole **8**, and isoxazoles (**9** and **10**) were potent in both cell free and in Molt-4 cell proteasome CT-L activity assays and were relatively insensitive to the MDR transporter. Methylation at the 5-position of 3-isoxazole **11** substantially improved its potency against the proteasome without affecting MDR sensitivity. Other substituents such as isopropyl **12** and methoxymethyl **13** at the same position were well tolerated but not significantly better than methyl group. In contrast, five-membered heterocycles containing an NH group such as pyrazole **14** and imidazole **15** showed similar potency but increased MDR sensitivity. Methylation on the nitrogen of the capping groups (**16**, **17**) but not other positions (e.g., **18**) made the analogues less MDR sensitive. N-Containing six-membered heterocycles such as 4-pyridine **19** and 4-pyridazine **20** displayed adequate potency against the proteasome but were MDR sensitive despite the absence of hydrogen attached to the nitrogen. Compound **21** was a very poor proteasome inhibitor even though it shares the same N-cap (2-pyrazine), P1, and P2 with bortezomib. Nonaromatic heterocycles such as tetrahydrofurans (**22**, **23**) were well tolerated as N-cap. Urea-linked N-caps (e.g., **24**) were also potent but increased sensitivity of the compounds to MDR activity. While a number of N-cap variants exhibit favorable potency, cell permeability, and MDR insensitivity, none were soluble enough to be formulated for oral administration (i.e., ≥1.0 mg/mL in the aforementioned EtOH/PS80/citrate vehicle; see solubility data of representative analogues listed in Table S1 of the Supporting Information). Therefore, two approaches were chosen to increase solubility of compound **11**, the compound

displaying the most favorable combination of potency and MDR insensitivity: (a) introduction of solubility-enhancing substituents at the 5-position of 3-isoxazole, and (b) modification of the peptide backbone of 5-Me-3-isoxazole-Leu-Phe-Leu-ketoepoxide.
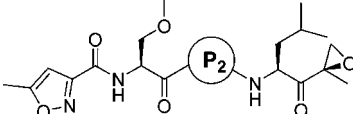
A set of solubilizing groups were attached to the 5-position of 3-isoxazole through a methenyl group, and the resulting potent analogues are listed in Table 3. Introduction of triazole **25**, imidazole **26**, N-Me-piperazine **27**, and morpholine **28** resulted in solubility sufficient for oral administration (i.e., ≥1.0 mg/mL). Among them, compound **28** was able to promote significant proteasome inhibition in peripheral tissues such as adrenal after po dosing. However, compounds (**25**, **26**, and **27**) did not display oral bioactivity, perhaps due in part to their high MDR sensitivity.

P3 Modification. A set of 30 natural and non-natural amino acids were tested at the P3 position with either 5-methyl or 5-morpholinomethyl 3-isoxazole as the N-cap. Representative analogues with potent in vitro activity are also listed in Table 3. P3 substituents containing ether and heterocyclic amino acids had improved solubility relative to leucine (Table S1 of the Supporting Information). Analogues with 5-methyl-3-isoxazole as N-cap (**11**, **29**, **31**, **33**, **35**, **37**, and **39**) demonstrated reduced MDR sensitivity and equivalent or greater oral bioactivity as compared to their morpholinomethyl counterparts (**28**, **30**, **32**, **34**, **36**, **38**, and **40**, respectively). When comparing across P3 analogues, those with low stability in SIF, such as 4-thiazolylalanine (**31**, **32**) and 2-pyridylalanine (**35**, **36**) showed the least oral bioactivity. Conversely, P3 analogues with methylserine (**29**, **30**) and homomethylserine (**33**, **34**) were highly stable in SIF and demonstrated increased oral bioactivity. Most of these analogues, however, were rapidly degraded in liver microsomes across multiple species ($R_e > 0.85$, data not shown). Among the P3 substitutions, compound **29** displayed the best in vitro and in vivo properties; therefore, 5-methyl-3-isoxazole and

Table 3. Solubility-Enhancing Substituents on 5-Position of 3-Isoxazole-Leu-Phe-Leu-Ketoepoxide and P3 Modification with 5-Me-3-Isoxazole-P3-Phe-Leu-Ketoepoxide

compd	R	P3	20S CT-L[a] IC$_{50}$ (nM)	Molt-4 CT-L[a] IC$_{50}$ (nM)	mice PO PD (% CT-L activity @ 40 mg/kg) adrenal[b]	MES cell viability ± MDR[a] IC$_{50}$ (nM) MDR−	MDR+	SIF stability (% parent @ 15 min)
25	1-(1,2,4)-triazole-CH$_2$	Leu	13	62	105	35	>1000	ND[e]
26	1-imidazole-CH$_2$	Leu	15	59	110	52	>1000	ND[e]
27	N-Me-piperazine-CH$_2$	Leu	94	124	101	189	>1000	40
11	Me	Leu	1.8 ± 0.9 (5)	17 ± 12 (5)	ND[c]	28 (22, 34)	47 (32, 64)	60
28	morpholine-CH$_2$	Leu	4.1	11 ± 3 (3)	29	22 ± 8 (3)	70 ± 20 (3)	60
29	Me	Ser(OMe)	9.3 ± 5.9 (3)	36 ± 14 (3)	9	40 (31, 48)	75 (53, 96)	90
30	morpholine-CH$_2$	Ser(OMe)	5.7	26 (15, 37)	57	13	147	80
31	Me	(4-Thiazolyl)-ala	6.7 (5.1, 8.4)	56 (46, 66)	63@10[d]	15	77	20
32	morpholine-CH$_2$	(4-Thiazolyl)-ala	6.9 (6.1, 7.6)	59	93	7.9	841	15
33	Me	hSer(OMe)	26 (19, 33)	69 (58, 80)	47	164	286	80
34	morpholine-CH$_2$	hSer(OMe)	19 (17, 20)	42	81	24	1145	90
35	Me	(2-Py)-ala	13	78	23	45	219	20
36	morpholine-CH$_2$	(2-Py)-ala	5.2	31	92	11	421	20
37	Me	(3-Py)-ala	1.6	27	70	39	543	90
38	morpholine-CH$_2$	(3-Py)-ala	6.4 ± 3.6 (3)	30	90	17	>1000	70
39	Me	(4-Py)-ala	2.8	8.6	28	8.6	271	90
40	morpholine-CH$_2$	(4-Py)-ala	5.1	14	96	8.7	>1000	60

[a] All experiments to determine IC$_{50}$ values were run with at least duplicates at each compound dilution; IC$_{50}$ values were averaged when determined in two or more independent experiments; the individual IC$_{50}$ values listed in parentheses ($n = 2$) or ± standard deviation denoted and n listed in parentheses ($n \geq 3$). [b] Adrenal selected as the peripheral tissue and inhibition in blood always equivalent or better than adrenal. [c] Not determined due to its poor solubility. [d] Dosed at 10 mg/kg. [e] Not determined.

Table 4. P2 Modification with 5-Me-3-Isoxazole-Ser(OMe)-P2-Leu-Ketoepoxide

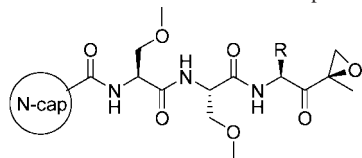| compd	P2	20S CT-L[a] IC$_{50}$ (nM)	Molt-4 CT-L[a] IC$_{50}$ (nM)	mice PO PD (% CT-L activity @ 20 mg/kg), adrenal	MES cell viability ± MDR[a] IC$_{50}$ (nM) MDR−	MDR+	SIF stability (% parent @ 15 min)	liver microsome stability (R_e) mouse	human
29	Phe	9.3 ± 5.9 (3)	36 ± 14 (3)	33	40 (31, 48)	75 (53, 96)	90	0.96	0.91
41	cyhxy-ala	13	78	56	210	353	75	0.96	0.94
42	3-thienyl-ala	9.2	46	117	25	181	90	0.95	0.87
43	4-thiazolyl-ala	16 ± 3 (3)	25 ± 23 (3)	39	17 ± 2 (5)	367 ± 124 (5)	100	0.86	0.85
44	Val	44	147	12	57	636	95	0.79	0.63
45	Leu	20	41	37	45	366	90	0.45	0.83
46	Ala	19 ± 5 (6)	57 ± 28 (3)	8	28 ± 5 (5)	276 ± 57 (5)	100	0.48	0.28
47	Abu	54	248	90	92	468	100	0.47	ND[b]
48	CN-Ala	40	91	40	29	941	100	0.28	ND[b]
49	Ser(OMe)	11 ± 4 (10)	48 ± 26 (3)	9	22 ± 2 (4)	145 ± 52 (4)	70	0.67	0.54

[a] All experiments to determine IC$_{50}$ values were run with at least duplicates at each compound dilution; IC$_{50}$ values were averaged when determined in two or more independent experiments; the individual IC$_{50}$ values listed in parentheses ($n = 2$) or ± standard deviation denoted and n listed in parentheses ($n \geq 3$). [b] Not determined.

methylserine were selected as N-cap and P3, respectively, for further optimization.

P2 Modification. A similar set of 30 natural and non-natural amino acids were chosen for P2 modification, and representative potent analogues are outlined in Table 4. Although most of these compounds were stable in SGF and SIF, they differed in sensitivity to first pass metabolic pathways. Bulky amino acids at P2 such as phenylalanine (**29**), cyclohexylalanine (**41**), 3-thienylalanine (**42**), 4-thiazolylalanine (**43**), and even valine (**44**) and leucine (**45**) resulted in compounds that were unstable in liver microsomal assays. On the other hand, compounds with small amino acids at P2 such as alanine (**46**), 2-aminobutyric acid (Abu) (**47**), cyanoalanine (**48**), and methylserine (**49**) were more resistant to microsomal degradation. Consequently, with

the exception of analogue **47**, these analogues demonstrated greater oral bioactivity. In addition, compound **49** displayed better solubility (Table S1 of the Supporting Information). On the basis of these results, 5-methyl-3-isoxazole was kept as N-cap and methylserine was chosen as both P2 and P3 for further optimization.

P1 Modification and N-Cap Rescreening. Carfilzomib is >100 fold selective for the CT-L activity versus either the T-L and C-L activities and mediates an equivalent inhibition of β5 and LMP7. We utilized an ELISA-based active site binding assay with intact cells to profile the active site selectivity of selected analogues.[34] Most of the tripeptidyl analogues with leucine as P1 (**50**, **49**, **53**, **55**, and **57**) displayed greater potency for β5 than LMP7, making these compounds selective for the

Table 5. Subunit Profile Comparison of Leu and Phe as P1 with Methylserine as Both P2 and P3 and Variant N-Caps

compd	N-cap	R[a]	ELISA-based active site IC$_{50}$[b] (nM)	
			β5	LMP7
50	3-isoxazole	*i*-Bu	48 ± 31 (3)	607 ± 273 (3)
51	3-isoxazole	CH$_2$Ph	44	93
49	5-Me-3-isoxazole	*i*-Bu	17 ± 10 (5)	238 ± 114 (5)
52	5-Me-3-isoxazole	CH$_2$Ph	11 (8.2, 13)	21 (15, 27)
53	5-EtO-3-isoxazole	*i*-Bu	9.3 (5.4, 13)	41 (40, 42)
54	5-EtO-3-isoxazole	CH$_2$Ph	3.7 (1.9, 5.4)	5.0 (2.7, 7.3)
55	3-MeO-5-isoxazole	*i*-Bu	23 (20, 25)	22 (17, 28)
56	3-MeO-5-isoxazole	CH$_2$Ph	14 (14, 14)	36 (36, 37)
57	2-Me-5-thiazole	*i*-Bu	73	784
58	2-Me-5-thiazole	CH$_2$Ph	36	82
2	−	−	5.2 ± 2.5 (27)	14 ± 9 (27)
1	−	−	8.7 ± 4.6 (6)	8.1 ± 5.4 (6)

[a] Leu: R=*i*-Bu; Phe: R=CH$_2$Ph. [b] All experiments to determine IC$_{50}$ values were run with at least duplicates at each compound dilution; IC$_{50}$ values were averaged when determined in two or more independent experiments; the individual IC$_{50}$ values listed in parentheses (*n* = 2) or ± standard deviation denoted and n listed in parentheses (*n* ≥ 3).

constitutive proteasome (Table 5). Previous reports have indicated that tetrapeptide-based proteasome inhibitors with phenylalanine as P1 may enhance inhibition of LMP7 (the CT-L activity of the immunoproteasome).[39,40] Therefore, we investigated the impact of leucine versus phenylalanine substitutions at P1 in a series of compounds. Tripeptide analogues with phenylalanine as P1 (**51**, **52**, **54**, **56**, and **58**) demonstrated an equivalent potency for β5 and LMP7 (Table 5). Similar to carfilzomib, these analogues also displayed selectivity for the CT-L subunits over T-L and C-L activities of the proteasome (data not shown). Furthermore, these P1 phenylalanine analogues exhibited similar in vitro potency, MDR sensitivity, and stability as compared to their P1 leucine counterparts (Table 6). Most importantly, the P1 phenylalanine and leucine analogues displayed similar oral bioactivity. Two analogues, 5-EtO-3-isoxazole (**54**) and 2-Me-5-thiazole (**58**) (PR-047), from an N-cap rescreening within the Ser(OMe)-Ser(OMe)-Phe-ketoepoxide backbone series, were selected for further in vivo efficacy, PK, and PD testing based on their oral bioactivity.

Antitumor Activity, Absolute Bioavailability, and PD Kinetics. Carfilzomib has been shown to mediate antitumor responses in multiple mouse models of cancer.[22,23] We evaluated the antitumor activity of the lead compounds (**54**, **58**) along with carfilzomib in immunocompromised mice bearing established xenografts of the Non-Hodgkin's lymphoma cell line RL and in BALB/c mice bearing the mouse colorectal tumor cell line CT-26. When each compound was administered on a weekly QD×2 schedule (Figure 3), compound **58** (po administered) promoted an equivalent antitumor response to carfilzomib (iv administered) in both models. However, **54** (po administered) was not able to achieve significant antitumor response in either model (further statistical analysis of antitumor responses are listed in Table S2 of the Supporting Information). It is noteworthy that **58** was administered below its maximum tolerated dose (MTD), while carfilzomib and **54** were delivered at their respective MTDs.

Compound **58** displayed a moderate absolute oral bioavailability (*F*) across multiple species by plasma PK measurement and blood PD measurement (Table 7). In mice, PD bioactivity

was calculated by comparing dose response curves for proteasome inhibition in blood following po and iv administrations. Oral bioactivity measured by PK and PD was found to be comparable, which reconfirmed the rationale that measurement of PD (CT-L activity 1 h postdose) following po administration can be used as a primary screening assay to evaluate bioactivity and bioavailability (*F*) of this series of peptide epoxyketone analogues.
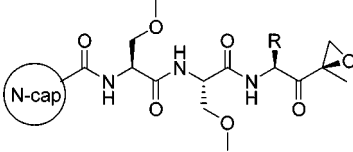
Because peptide epoxyketone proteasome inhibitors are irreversible, their absolute potency is most accurately described by their inactivation kinetics (k_{inact}/K_i). The k_{inact}/K_i for a subset of key compounds (Table S3 of the Supporting Information) demonstrated that rapid inactivation of the target was well correlated with the relative potency reflected by IC$_{50}$ values measured at 1 h with purified enzyme and on cells. Furthermore, the IC$_{50}$ values of the all set of epoxyketone analogues for CT-L inhibition in Molt-4 cells are also directly proportional to cellular cytotoxicity (data not shown). Thus, the determination of IC$_{50}$ values at a fixed time point (1 h) provides an efficient screening strategy for defining the relative potency of analogues. Furthermore, the kinetics of proteasome inhibition in animals following po administration of **58** demonstrated rapid absorption, tissue distribution, and inactivation of the proteasome (Figure 4). Within 15 min of dosing, proteasome inhibition in excess of 80% was achieved in blood and all tissues examined except the brain. This rapid onset of proteasome inhibition is comparable to that seen with iv administration of carfilzomib.[22,23] Similar to carfilzomib, proteasome activity recovered through new proteasome synthesis in all tissues, with the exception of blood, within 24−72 h.

Conclusions

Although a variety of peptide-based drugs have been commercialized successfully, most of these therapeutics are administered by the parenteral route because of insufficient oral bioavailability.[38] Furthermore, epoxides are typically chemically reactive and unstable in low pH environments,[41] presenting an additional challenge to the identification of orally active peptidyl epoxyketone proteasome inhibitors. Through a systematic SAR optimization and in vivo PD screening effort, we improved solubility, metabolic stability (gastric fluid, intestinal fluid, liver microsomes, and hepatocytes), and sensitivity to the multidrug resistance protein 1 (MDR1) and, most importantly, oral bioavailability in this series of compounds. These efforts culminated in the identification of **58**, a compound that promoted antitumor activity in multiple animal models by oral administration at doses below the MTD. Taken together, the data presented here demonstrate that **58** is an orally bioavailable and selective proteasome inhibitor with favorable pharmacologic properties and support the further development of this molecule for the treatment of malignant diseases.

Synthesis

The generalized route for the synthesis of peptide epoxyketone, exemplified by synthesis of **58**, is illustrated in Schemes 1 and 2.[40,42,43] Cbz-protected phenylalanine **59** was converted into the Weinreb amide **60**, followed by treatment with Grignard reagent to yield enone **61**. The enone was then reduced with sodium boronate and cerium(III) chloride into alcohols **62a** (2*S*,3*R*) and **62b** (2*S*,3*S*) in a ratio of 6/1. The mixed allylic alcohols were treated with *tert*-butylhydroperoxide in the presence of vanadyl acetylacetonate as catalyst to achieve allylic epoxides **63a** (1*R*,2*S*,3*S*) and **63b** (1*S*,2*R*,3*S*) in a similar ratio. These allylic epoxides are unstable and were oxidized directly

Table 6. P1 and N-Cap Modification with Methylserine as Both P2 and P3

compd	N-cap	R^a	20S CT-L[b] IC_{50} (nM)	Molt-4 CT-L[b] IC_{50} (nM)	mice PO PD (% CT-L activity @ 10 mg/kg), adrenal	MES cell viability ± MDR[b] IC_{50} (nM) MDR−	MDR+	SIF stability (% parent @ 15 min)	liver microsome stability (R_e) mouse	human
50	3-isoxazole	*i*-Bu	43 ± 8 (3)	168	14	37	260	90	0.39	0.16
51	3-isoxazole	CH₂Ph	73	47	34	43	756	85	0.49	0.42
49	5-Me-3-isoxazole	*i*-Bu	11 ± 4 (10)	48 ± 26 (3)	21	22 ± 2 (4)	145 ± 52 (4)	70	0.67	0.54
52	5-Me-3-isoxazole	CH₂Ph	24 ± 6 (3)	35 (24, 45)	43	17 (12, 21)	155 (139, 171)	90	0.59	0.59
53	5-EtO-3-isoxazole	*i*-Bu	3.1 ± 0.3 (3)	35	4	5.4 (4.2, 6.5)	66 (39, 94)	70	0.69	0.69
54	5-EtO-3-isoxazole	CH₂Ph	1.4	3.0	3	4.3	54	85	0.77	0.77
55	3-MeO-5-isoxazole	*i*-Bu	11 ± 6 (3)	32	21	12	82	35	0.37	0.40
56	3-MeO-5-isoxazole	CH₂Ph	50 (45, 56)	10	19	12	269	100	0.54	0.64
57	2-Me-5-thiazole	*i*-Bu	74	164	45	38	1157	80	0.21	0.41
58	2-Me-5-thiazole	CH₂Ph	55 ± 19 (9)	66	6	25 ± 15 (4)	1322 ± 316 (4)	90	0.51	0.60

[a] Leu: R=*i*-Bu; Phe: R=CH₂Ph. [b] All experiments to determine IC_{50} values were run with at least duplicates at each compound dilution; IC_{50} values were averaged when determined in two or more independent experiments; the individual IC_{50} values listed in parentheses ($n = 2$) or ± standard deviation denoted and n listed in parentheses ($n \geq 3$).
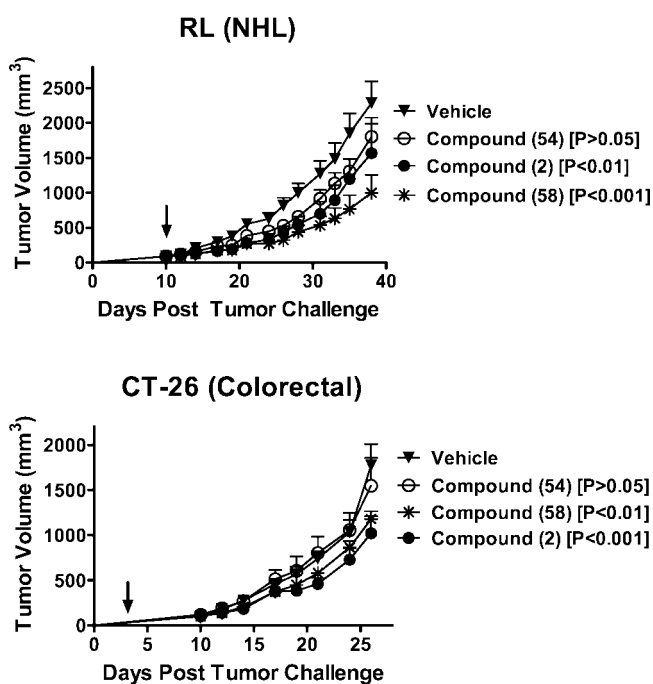
Figure 3. Antitumor activity of compounds **2**, **54**, and **58**. BNX mice bearing established human tumor xenografts derived from RL and BALB/c mice challenged with the murine tumor cell line CT-26 were treated twice weekly on days 1 and 2 (QD×2) with 5 mg/kg **2** (iv), 20 mg/kg **54** (po), or 30 mg/kg **58** (po). Arrow indicates the start of dose period. Data are presented as mean tumor volume ± SEM ($n = 8-10$/group). Statistical comparisons between treatment groups and vehicle controls were made by two-way ANOVA followed by Bonferroni post hoc analysis (Table S2, Supporting Information). *P* values reflect the statistical significance by the end of study.

Table 7. Oral Bioavailability (*F*) of Compound **58**

	mouse	rat	dog
F calculated by PK (Dose)	17 (40 mg/kg)	21 (40 mg/kg)	39 (19 mg/kg)
F calculated by PD	36[a]	−	−

[a] iv dose range: 1−5 mg/kg; po dose range: 5−20 mg/kg.

into epoxyketones with Dess−Martin reagent. The major isomer **64a** (1*R*,3*S*) was isolated from others by flash chromatography. Benzyl ester-protected methylserine **67** was prepared from Boc-protected methylserine **65** with benzyl chloroformate followed

by deprotection of Boc group.[44] Dipeptide BocNH-Ser(OMe)-Ser(OMe)-OBn (**68**) was then prepared by coupling of protected methylserines **65** and **67** under a condition of HOBt, HBTU, and DIEA. Similarly, 2-Me-thiazol-5-yl-Ser(OMe)-Ser(OMe)-OBn (**71**) was prepared from coupling of 2-methylthiazole-5-carboxylic acid and intermediate **69**. However, hydrogenation of **71** using Pd/C to remove benzyl ester group failed to yield acid **72**, most likely due to poisoning of the catalyst by thiazole. In contrast, hydrogenation under the same condition to remove the benzyl ester group of dipeptide **68** yielded acid **73** quantitatively. Removal of Cbz group from **64a** by hydrogenation with Pd/C in trifluoroacetic acid (TFA) resulted in TFA salt **74**, which was then coupled with acid **73** into Boc-Ser(OMe)-Ser(OMe)-Phe-ketopoxide (**75**). The latter was treated with TFA to remove Boc group and coupled with 2-methylthiazole-5-carboxylic acid under a condition of HOBt, HBTU, and DIEA to yield the target molecule **58**.

Experimental Section

General Methods. Chemicals, reagents and solvents were obtained from commercial sources and used as received. NMR spectra were obtained on a Varian Mercury-300 spectrometer in the indicated solvents. Analytical LCMS was run on Water 2996 eluting with a mixture of acetonitrile and water containing 0.1% acetic acid. Mass spectra were obtained using Water EMD1000 mass spectrometer, and UV absorption was recorded at wavelength of 214 nm. Preparative reverse phase HPLC was run using Water 2695 instrument with a YM 25 cm × 50 mm column eluting with a mixture of acetonitrile and water containing 0.1% ammonium acetate. Normal phase flash chromatography was performed on silica gel 60.

Benzyl (*S*)-1-(*N*-Methoxy-*N*-methylcarbamoyl)-2-phenylethylcarbamate (60). A suspension of *N*,*O*-dimethylhydroxylamine hydrochloride (41.0 g, 420 mmol) in DCM (700 mL) was stirred vigorously for 0.5 h and then TEA (42.5 g, 420 mmol) was added via an addition funnel. In a separate flask, to a 0 °C solution of Cbz-phenylalanine (**59**) (125.0 g, 420 mmol) in DCM (700 mL) was added isobutylchloroformate (57.3 g, 420 mmol) dropwise via an addition funnel, and the resulting mixture was further cooled to −20 °C and NMM (42.5 g, 420 mmol) was added via an addition funnel at such a rate to maintain the temperature below −10 °C. The freshly prepared dimethyl hydroxylamine solution was then added via a wide bore Teflon canula at a rate to maintain the temperature below −5 °C. The reaction mixture was warmed to room temperature for 1.5 h followed by dilution with water (500
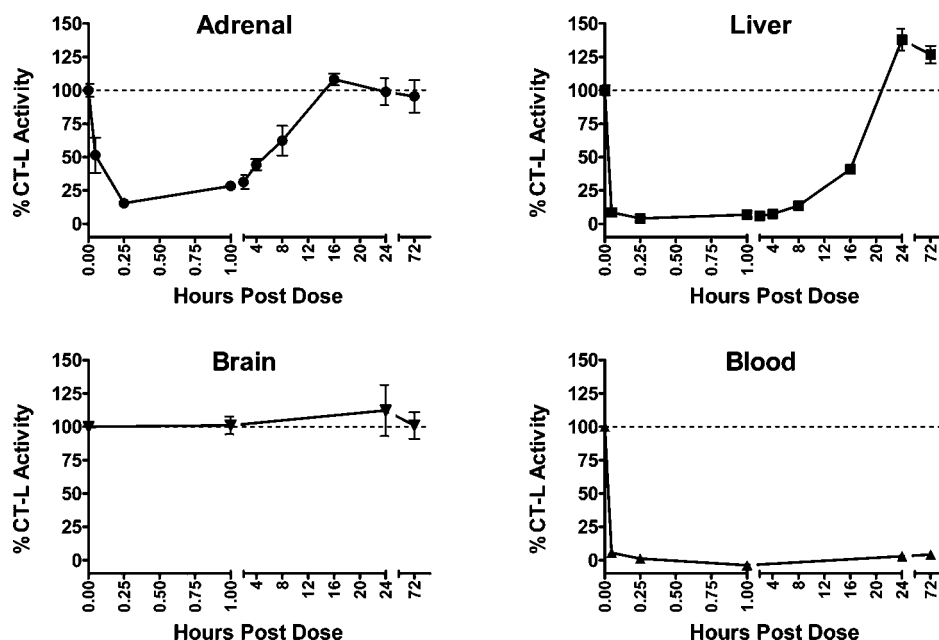
Figure 4. Kinetics of proteasome inhibition following po administration of compound **58**. BALB/c mice (n = 3/time point) received a single po administration of 30 mg/kg, and proteasome inhibition was measured at the indicated time points using LLVY-AMC substrate. Data are presented as mean residual activity ($\pm$SEM) relative to vehicle treated controls.

**Scheme 1.** Generalized Route to Synthesize Cbz-Phe Epoxyketone [a]
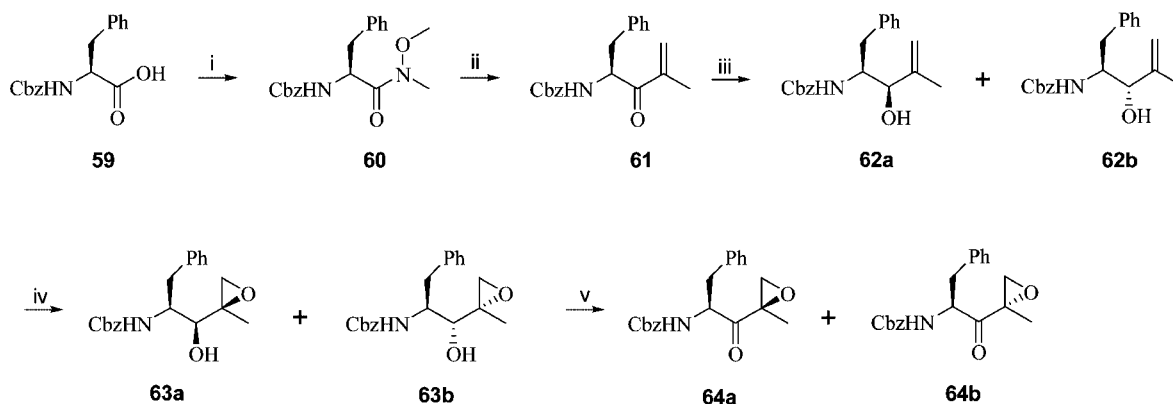
[a] Reagents and conditions: (i) *i*-BuOCOCl, NMM, *N*,*O*-dimethylhydroxylamine hydrochloride, TEA, DCM, −20 °C; (ii) isopropenylmagnesium bromide, THF, 0 °C; (iii) NaBH$_4$, CeCl$_3$·7H$_2$O, MeOH, THF, 0 °C−rt; (iv) vanadyl acetylacetonate, *t*-BuO$_2$H, DCM, 0 °C; (v) Dess−Martin periodinane, DCM, 0 °C−rt.

mL). The layers were separated, and the aqueous layer was extracted with DCM (2 × 150 mL). The combined organic layers were washed with 1 N HCl (4 × 500 mL), water (1 × 150 mL), aqueous NaHCO$_3$ solution (4 × 150 mL), brine (1 × 250 mL), and dried over Na$_2$SO$_4$. The Na$_2$SO$_4$ was removed by filtration, and the volatiles were removed under reduced pressure to give Weinreb amide **60** (166 g). LRMS (M + H$^+$) *m/z*: calcd 343.16; found 343.16. ^{1}H NMR (300.05 MHz, CDCl$_3$): δ 2.91 (dd, J = 7.2, 13.8 Hz, 1H, CHCH$_2$Ph), 3.08 (dd, J = 5.8, 13.8 Hz, 1H, CHCH$_2$Ph), 3.17 (s, 3H, NCH$_3$), 3.68 (s, 3H, OCH$_3$), 5.00−5.11 (m, 3H, OCH$_2$Ph + NHCH), 5.45 (d, J = 8.8 Hz, 1H, NHCH), 7.12−7.38 (m, 10H, 2C$_6$H$_5$).

Benzyl (*S*)-4-Methyl-3-*oxo*-1-phenylpent-4-en-2-ylcarbamate (61). To a 0 °C solution of the isopropenyl magnesium bromide (2 L, 1000 mmol, 0.5 M solution in THF) was added a solution of amide **60** (116.0 g, 484 mmol) in dry THF (1 L) dropwise via an addition funnel under an atmosphere of argon. The reaction was stirred at 0 °C for 6 h and then slowly poured into a beaker containing 1.25 L of saturated NH$_4$Cl solution and approximately 1.25 L of ice. The pH of the solution was adjusted to 1.5 using concentrated HCl when all the ice melted, and the resulting mixture was extracted with EtOAc (2 × 2 L). The combined organic layers

were washed with aqueous NaHCO$_3$ solution (1 × 1 L), brine (1 × 1 L), and dried over MgSO$_4$. The MgSO$_4$ was removed by filtration, and the volatiles were removed under reduced pressure. Purification of residue by flash chromatography gave enone **61** (103.3 g, 76% over the first two steps) as oil. LRMS (M + H$^+$) *m/z*: calcd 324.15; found 324.15. ^{1}H NMR (300.05 MHz, CDCl$_3$): δ 1.86 (s, 3H, CCH$_3$), 2.97 (dd, J = 6.0, 13.8 Hz, 1H, CHCH$_2$Ph), 3.15 (dd, J = 6.3, 13.8 Hz, 1H, CHCH$_2$Ph), 5.09 (dd, J = 12.4, 18.2 Hz, 2H, OCH$_2$Ph), 5.35 (dd, J= 6.0, 14.03 Hz, 1H, NHCH), 5.58 (d, J = 8.0 Hz, 1H, NHCH), 5.89 (br s, 1H, C=CH$_2$), 6.04 (br s, 1H, C=CCH$_2$), 7.01−7.39 (m, 10H, 2C$_6$H$_5$).

Benzyl (2*S*,3*R*)-3-Hydroxy-4-methyl-1-phenylpent-4-en-2-yl-carbamates (62a, 62b). To a 0 °C solution of compound **61** (103.3 g, 320 mmol) in MeOH (1.3 L) and THF (1.3 L) was added CeCl$_3$·7H$_2$O (172.6 g, 463 mmol) under an atmosphere of argon. Then NaBH$_4$ (17.5 g, 463 mmol) was added once it became homogeneous. The reaction mixture was stirred at the same temperature for 6 h and quenched with glacial acetic acid (230 mL). The resulting mixture was stirred until homogeneous. The volatiles were removed under reduced pressure, and the remaining oil was diluted with water (1 L) and extracted with EtOAc (3 × 500 mL). The combined organic layers were washed with water (2 × 500

Scheme 2. Generalized Route to Synthesize Tripeptide Epoxyketone **58**[a]
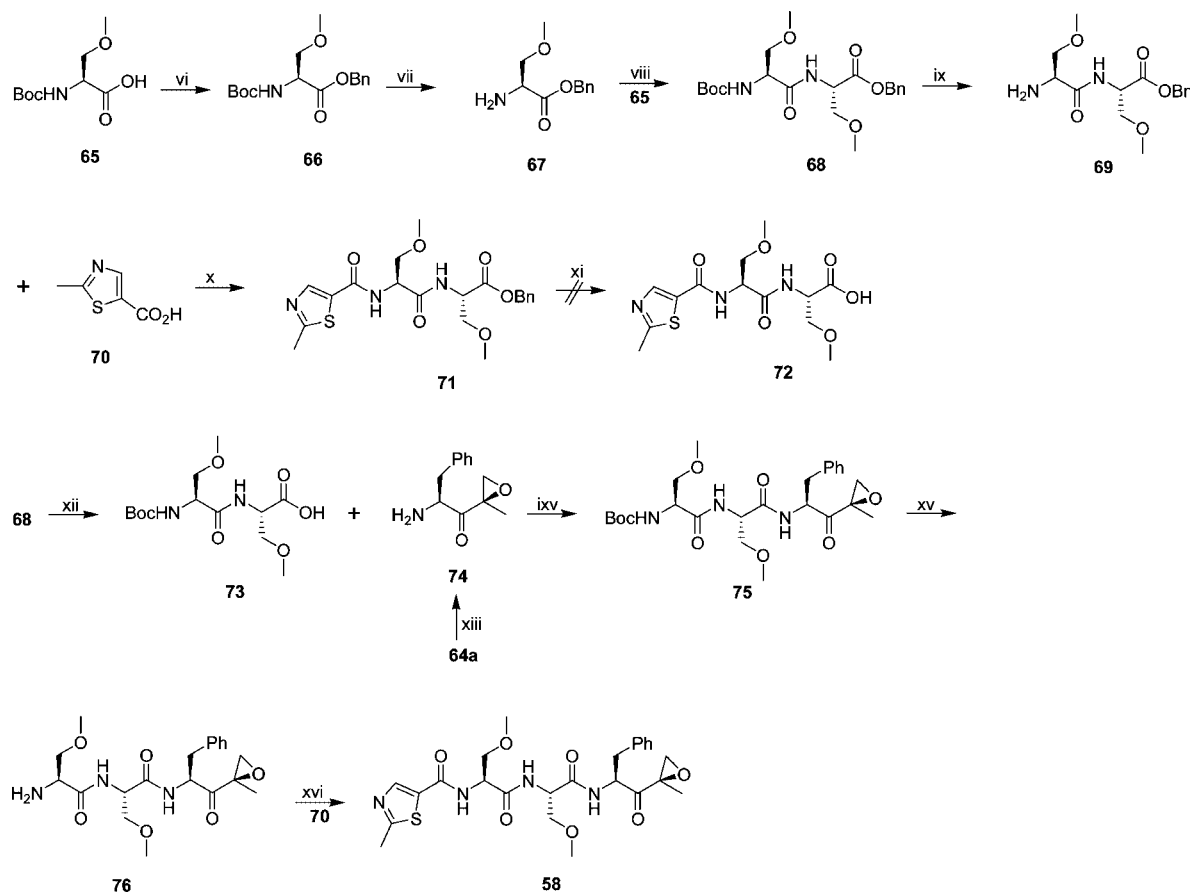
[a] Reagents and conditions: (vi) BnOCOCl, TEA, DMAP, DCM, 0 °C; (vii) TFA, DCM, rt; (viii) **65**, HOBt, HBTU, DIEA, THF, 0 °C; (ix) TFA, DCM, 0 °C; (x) HOBt, HBTU, DIEA, THF, 0 °C; (xi) THF, Pd/C, H₂, rt; (xii) THF, Pd/C, H₂, rt; (xiii). TFA, Pd/C, H₂, rt; (xiv) HOBt, HBTU, DIEA, THF, 0 °C; (xv) TFA, DCM, 0 °C; (xvi) **70**, HOBt, HBTU, DIEA, THF, 0 °C.

mL), brine (2 × 500 mL), and dried over MgSO₄. The MgSO₄ was removed by filtration, and the volatiles were removed under reduced pressure to give a mixture of compounds (**62a**, **62b**) (102.5 g, 98%, ratio 6:1 based on LCMS analysis) as oil. LRMS (M + H⁺) *m/z*: calcd 326.17; found 326.17. ¹H NMR (300.05 MHz, CDCl₃): δ 1.68 (s, 3H, CCH₃, minor isomer), 1.82 (s, 3H, CCH₃, major isomer), 2.02 (br s, 1H, OH), 2.91 (dd, *J* = 3.3, 14.2 Hz, 2H, CHCH₂Ph), 3.97−4.20 (br s, 2H, NHCH + CHOH), 4.90−5.07 (m, 5H, NHCH + OCH₂Ph + C=CCH₂), 7.15−7.33 (m, 10H, 2C₆H₅).

Benzyl (*S*)-1-((*R*)-2-Methyloxiran-2-yl)-1-*oxo*-3-phenylpropan-2-ylcarbamate (64a). To a 0 °C solution of alcohols (**62a**, **62b**) (102.5 g, 300 mmol) in dry DCM (300 mL) was added VO(acac)₂ (2.9 g, 10.7 mmol) under an atmosphere of argon. Then *t*-BuO₂H (105.5 mL, 580 mmol, 5.5 M solution in decane) was added dropwise via an addition funnel. The reaction was warmed to room temperature for 6 h and became light yellow. The resulting mixture was filtered through celite, and the layers were separated. The aqueous layer was extracted with DCM (2 × 100 mL). The combined organic layers were washed with aqueous sodium bisulfite solution (2 × 200 mL), brine (2 × 200 mL), and dried over Na₂SO₄. The Na₂SO₄ was removed by filtration, giving a DCM solution of intermediates (**63a**, **63b**), which were used in the next step. LRMS (M + H⁺) *m/z*: calcd 342.16; found 342.16.

To a 5 °C solution of aforementioned intermediates (**63a**, **63b**) in DCM (2.5 L) was added Dess−Martin periodinane (316 g, 16.4 mmol) in DCM (1 L) under an atmosphere of argon. The reaction was kept at room temperature overnight. The resulting mixture was cooled in an ice-bath, diluted with aqueous NaHCO₃ solution (1 L), and EtOAc (2 L), and filtered through celite. The layers were separated and the aqueous layer was extracted with EtOAc (2 × 1

L). The combined organic layers were washed with water (3 × 1 L), brine (1 × 1 L), and dried over MgSO₄. The MgSO₄ was removed by filtration, and the volatiles were removed under reduced pressure to give crude residue as oil. Purification by flash chromatography with ethyl acetate/hexane gave epoxyketone (**64a**) (38.7 g, 27% yield of the two-step). LRMS (M + H⁺) *m/z*: calcd 340.15; found 340.15. ¹H NMR (300.05 MHz, CDCl₃): δ 1.52 (s, 3H, CH₃), 2.78 (dd, *J* = 7.7, 14.0 Hz, 1H, CHCH₂Ph), 2.93 (d, *J* = 5.0 Hz, 1H, OCH₂), 3.14 (dd, *J* = 5.1, 13.9 Hz, 1H, CHCH₂Ph), 3.30 (d, *J* = 5.0 Hz, 1H, OCH₂), 4.66 (ddd, *J* = 5.0, 8.0, 12.4 Hz, 1H, NHCH), 5.03 (dd, *J* = 12.4, 14.9 Hz, 2H, OCH₂Ph), 5.24 (d, *J* = 8.3 Hz, 1H, NHCH), 7.14−7.38 (m, 10H, 2C₆H₅).

***tert*-Butyl (*S*)-1-((Benzyloxy)carbonyl)-2-methoxyethylcarbamate (66).** To a solution of Boc-methylserine **65** (43.8 g, 200 mmol) in DCM (400 mL) were added TEA (26.5 g, 260 mmol) and DMAP (2.4 g, 20 mmol). The resulting solution was cooled to −5 °C, and benzyl chloroformate (41.0 g, 240 mmol) was then slowly added via an addition funnel under an atmosphere of argon. The reaction was kept at the same temperature for 3 h and then diluted with brine (100 mL). The layers were separated, and the aqueous layer was extracted with DCM (2 × 200 mL). The organic layers were combined and dried over Na₂SO₄. The Na₂SO₄ was removed by filtration, and the volatiles were removed under reduced pressure. The resulting residue was purified by flash chromatography using a mixture of hexane and ethyl acetate to provide intermediate **66** as white solid (54 g, 88% yield). LRMS (M + H⁺) *m/z*: calcd 310.16; found 310.16. ¹H NMR (300.05 MHz, CDCl₃): δ 1.44 (s, 9H, C(CH₃)₃), 3.29 (s, 3H, OCH₃), 3.60 (dd, *J* = 3.2, 9.3 Hz, 1H, CH₂OCH₃), 3.81 (dd, *J* = 3.1, 9.3 Hz, 1H, CH₂OCH₃), 4.45 (m, 1H, CHNH), 5.14 (d, *J* = 12.3 Hz, 1H,

CH$_2$Ph), 5.27 (d, J = 12.3 Hz, 1H, CH$_2$Ph), 5.40 (br s, 1H, NHCH), 7.26 (m, 5H, C$_6$H$_5$).

Benzyl (2S)-2-[(2S)-2-{[*tert*-Butoxy)carbonyl]amino}-3-methoxypropanamido]-3-methoxypropanoate (68). To a 0 °C solution of intermediate **66** in DCM (100 mL) was added TFA (100 mL) slowly via an addition funnel. The reaction was kept at the same temperature for 1 h, concentrated, and dried under high vacuum overnight. The resulting residual TFA salt **67** was used in the next step without further purification. LRMS (M + H$^+$) *m/z*: calcd, 210.11; found 210.1.

To a −5 °C mixture of aforementioned TFA salt **67**, Boc-methylserine **65** (36.7 g, 167 mmol), HOBt (27.0 g, 200 mmol), and HBTU (71.4 g, 200 mmol) in THF (600 mL) was added DIEA (76.6 g, 600 mmol) slowly via an addition funnel. The reaction was kept at the same temperature for 4 h, followed by dilution with EtOAc (500 mL) and brine (300 mL). The layers were separated, and the aqueous layer was extracted with EtOAc (2 × 300 mL). The organic layers were combined and dried over Na$_2$SO$_4$. The Na$_2$SO$_4$ was removed by filtration, and the volatiles were removed under reduced pressure. The resulting residue was purified by flash chromatography using a mixture of hexane and ethyl acetate to provide dipeptide **68** as white solid (65 g, 95% yield). LRMS (M + H$^+$) *m/z*: calcd 411.21; found 411.21. ^{1}H NMR (300.05 MHz, CDCl$_3$): δ 1.45 (s, 9H, C(CH$_3$)$_3$), 3.29 (s, 3H, OCH$_3$), 3.34 (s, 3H, OCH$_3$), 3.44 (dd, J = 6.9, 9.4 Hz, 1H, CH$_2$OCH$_3$), 3.61 (dd, J = 3.0, 9.4 Hz, 1H, CH$_2$OCH$_3$), 3.78 (dd, J = 3.9, 9.4 Hz, 1H, CH$_2$OCH$_3$), 3.84 (dd, J = 3.0, 9.4 Hz, 1H, CH$_2$OCH$_3$), 4.27 (m, 1H, CHNH), 4.75 (dt, J = 3.3, 6.3, 8.3 Hz, 1H, CHNH), 5.20 (q, J = 12.4, 28.6 Hz, 2H, CH$_2$Ph), 5.42 (br s, 1H, NH), 7.26 (m, 5H, C$_6$H$_5$).

Benzyl (2S)-3-Methoxy-2-[(2S)-3-methoxy-2-[(2-methyl-1,3-thiazol-5-yl)formamido]propanamido]propanoate (71). To a 0 °C solution of aforementioned intermediate **68** (18.0 g, 38 mmol) in DCM (100 mL) was added TFA (100 mL) slowly via an addition funnel. The reaction was kept at the same temperature for 2 h, concentrated, and dried under high vacuum overnight. The resulting residual TFA salt **69** was used in the next step without further purification. LRMS (M + H$^+$) *m/z*: calcd 311.15; found 311.15.

To a −5 °C mixture of TFA salt **69**, 2-methylthiazole-5-carboxylic acid (**70**) (5.8 g, 38 mmol), HOBt (6.8 g, 45 mmol), and HBTU (16.0 g, 45 mmol) in THF (600 mL) was added DIEA (10.0 g, 80 mmol) slowly. The reaction was kept at the same temperature for 4 h and then diluted with EtOAc (200 mL) and brine (200 mL). The layers were separated, and the aqueous layer was extracted with EtOAc (2 × 300 mL). The organic layers were combined and dried over Na$_2$SO$_4$. The Na$_2$SO$_4$ was removed by filtration, and the volatiles were removed under reduced pressure. The resulting residue was purified by flash chromatography using a mixture of hexane and ethyl acetate to provide benzyl ester **71** as white solid (14 g, 75% yield). LRMS (M + H$^+$) *m/z*: calcd 436.15; found 436.15. ^{1}H NMR (300.05 MHz, CDCl$_3$): δ 2.76 (s, 3H, CH$_3$-thiazole), 3.31 (s, 3H, OCH$_3$), 3.34 (s, 3H, OCH$_3$), 3.50 (dd, J = 8.3, 9.1 Hz, 1H, CH$_2$OCH$_3$), 3.63 (dd, J = 3.3, 9.6 Hz, 1H, CH$_2$OCH$_3$), 3.84 (dd, J = 4.1, 6.1 Hz, 1H, CH$_2$OCH$_3$), 3.87 (dd, J = 3.3, 5.5 Hz, 1H, CH$_2$OCH$_3$), 4.72 (m, 2H, 2CHNH), 5.20 (q, J = 12.4, 29.2 Hz, 2H, CH$_2$Ph), 7.06 (d, J = 6.6 Hz, 1H, NH), 7.35 (m, 5H, C$_6$H$_5$), 7.44 (d, J = 8.3 Hz, 1H, NH), 8.10 (s, 1H, H-thiazole).

***tert*-Butyl N-[(1S)-2-Methoxy-1-{[(1S)-2-methoxy-1-{[(2S)-4-methyl-1-[(2R)-2-methyloxiran-2-yl]-1-oxopentan-2-yl]carbamoyl]ethyl]carbamoyl}ethyl]carbamate (75).** A solution of dipeptide **68** (13.4 g, 32.7 mmol) in THF (200 mL) was stirred with Pd/C (2.7 g) under atmosphere of hydrogen for 2 h at room temperature. The Pd/C was then removed by filtration and washed with THF (100 mL). The volatiles were removed under reduced pressure. The residual acid **73** was dried and used in the next step without further purification. LRMS (M + H$^+$) *m/z*: calcd 321.16; found 321.16.

A 0 °C solution of aforementioned epoxyketone **64a** (8.0 g, 32.7 mmol) in TFA (80 mL) was stirred with Pd/C (2.0 g) under atmosphere of hydrogen for two hours. The Pd/C was removed by filtration and washed with DCM (50 mL). The volatiles were

removed under reduced pressure. The residual TFA salt **74** was dried over high vacuum and used in the next step without further purification. LRMS (M + H$^+$) *m/z*: calcd 206.11; found 206.11.

To a −5 °C mixture of the resulting acid **73** and epoxyketone TFA salt **74**, HOBt (6.0 g, 39.2 mmol), and HBTU (14.8 g, 39.2 mmol) in THF (600 mL) was added DIEA (23 mL) slowly via an addition funnel. The reaction was kept at the same temperature for 4 h, followed by dilution with EtOAc (200 mL) and brine (200 mL). The layers were separated, and the aqueous layer was extracted with EtOAc (2 × 300 mL). The organic layers were combined and dried over Na$_2$SO$_4$. The Na$_2$SO$_4$ was removed by filtration, and the volatiles were removed under reduced pressure. The resulting residue was purified by flash chromatography using a mixture of hexane and ethyl acetate to provide tripeptide **75** as white solid (9.2 g, 69% overall yield). LRMS (M + H$^+$) *m/z*: calcd 508.58; found 508.58. ^{1}H NMR (300.05 MHz, CDCl$_3$): δ 1.44 (s, 9H, C(CH$_3$)$_3$), 1.47 (s, 3H, CH$_3$-oxirane), 2.86 (dd, J = 7.5, 14.1 Hz, 1H, CH$_2$Ph), 2.88 (d, J = 4.5 Hz, 1H, CH$_2$ of oxirane), 3.11 (dd, J = 5.4, 14.1 Hz, 1H, CH$_2$Ph), 3.26 (d, J = 6.5 Hz, 1H, CH$_2$ of oxirane), 3.30 (s, 6H, 2OCH$_3$), 3.38 (dd, J = 6.0, 9.0 Hz, 1H, CH$_2$OCH$_3$), 3.46 (dd, J = 7.2, 9.0 Hz, 1H, CH$_2$OCH$_3$), 3.73 (dd, J = 3.9, 9.0 Hz, 1H, CH$_2$OCH$_3$), 3.78 (dd, J = 3.3, 9.0 Hz, 1H, CH$_2$OCH$_3$), 4.25 (m, 1H, CHNH), 4.43 (dq, J = 3.3, 6.0, 7.2, 9.3 Hz, 1H, CHNH), 4.86 (dt, J = 5.4, 7.5, 13.2 Hz, 1H, CHNH), 5.39 (d, J = 6.0 Hz, 1H, NH), 7.04−7.31 (m, 7H, C$_6$H$_5$ + 2NH).

(2S)-3-Methoxy-2-[(2S)-3-methoxy-2-[(2-methyl-1,3-thiazol-5-yl)formamido]propanamido]-N-[(2S)-1-[(2R)-2-methyloxiran-2-yl]-1-*oxo*-3-phenylpropan-2-yl]propanamide (58). To a 0 °C solution of intermediate **75** (18 g, 35 mmol) in DCM (100 mL) was added TFA (100 mL) slowly via an addition funnel. The reaction was kept at the same temperature for 2 h and concentrated under high vacuum. The resulting residual TFA salt **76** was dried overnight and used in the next step without further purification. LRMS (M + H$^+$) *m/z*: calcd 408.21; found 408.21.

To a −5 °C mixture of aforementioned TFA salt **76**, 2-methylthiazole-5-carboxylic acid **70** (5.8 g, 38 mmol), HOBt (6.8 g, 45 mmol), and HBTU (16.0 g, 45 mmol) in THF (600 mL) was added DIEA (10 g, 80 mmol) slowly via an addition funnel. The reaction was kept at the same temperature for 4 h and then diluted with EtOAc (200 mL) and brine (200 mL). The layers were separated, and the aqueous layer was extracted with EtOAc (2 × 300 mL). The organic layers were combined and dried over Na$_2$SO$_4$. The Na$_2$SO$_4$ was removed by filtration, and the volatiles were removed under reduced pressure. The resulting residue was purified by HPLC using a mixture of acetonitrile and aqueous NH$_4$Ac solution (0.1%) as mobile phases, and the desired product **58** (12 g, 64% yield) was isolated as white solid. LRMS (M + H$^+$) *m/z*: calcd 533.20; found 533.20. ^{1}H NMR (300.05 MHz, CDCl$_3$): δ 1.50 (s, 3H, CH$_3$-oxirane), 2.74 (s, 3H, CH$_3$-thiazole), 2.88 (dd, J = 7.2, 14.0 Hz, 1H, CH$_2$Ph), 2.91 (d, J = 5.0 Hz, 1H, CH$_2$ of oxirane), 3.14 (dd, J = 5.0, 14.0 Hz, 1H, CH$_2$Ph), 3.27 (d, J = 5.0 Hz, 1H, CH$_2$ of oxirane), 3.32 (s, 6H, 2OCH$_3$), 3.40 (dd, J = 5.8, 9.1 Hz, 1H, CH$_2$OCH$_3$), 3.55 (t, J = 8.8 Hz, 1H, CH$_2$OCH$_3$), 3.80 (d, J = 9.0 Hz, 1H, CH$_2$OCH$_3$), 3.81 (dd, J = 2.1, 9.3 Hz, 1H, CH$_2$OCH$_3$), 4.47 (dq, J = 3.0, 5.8, 7.4, 10.5 Hz, 1H, CHNH), 4.68 (dq, J = 4.4, 6.3, 8.3, 10.7 Hz, 1H, CHNH), 4.86 (dt, J = 5.5, 7.7, 12.9 Hz, 1H, CHNH), 6.92 (d, J = 6.1 Hz, 1H, NH), 7.08−7.31 (m, 7H, C$_6$H$_5$ + 2NH), 8.06 (s, 1H, H-thiazole). ^{13}C NMR (75.46 MHz, CDCl$_3$): δ 16.80, 19.90, 52.70, 52.74, 53.13, 59.32, 59.44, 59.52, 71.43, 71.71, 127.25, 128.68, 129.73, 133.41, 135.90, 143.88, 160.66, 169.60, 169.80, 170.95, 207.38. Elemental analysis (C$_{25}$H$_{32}$N$_4$O$_7$S, 532.61), found (calcd), C: 56.47 (56.38); H: 6.06 (5.74); N: 10.55 (10.52).

Other analogues were prepared through similar procedures. ^{1}H NMR and ^{13}C NMR spectra of representative compounds were listed in Supporting Information. All of these compounds possess a purity of not less than 95% (Table S4 of the Supporting information).

Supporting Information Available: Experimental details on biological assays, DMPK assays, animal studies, spectral characterization of compounds **5**, **11**, **28**, **29**, **49**, and **54** (including ^{1}H

NMR, ^{13}C NMR spectra), HPLC purity and solubility data, as well as inactivation rates (K_{inact}/K_i) of compounds **5**, **11**, **28**, **29**, **46**, **49**, **54**, and **58**, and statistical analysis of antitumor response (2-way ANOVA) of compounds **2**, **54**, and **58**. This material is available free of charge via the Internet at http://pubs.acs.org.

References

(1) Ciechanover, A. Proteolysis: From the Lysosome to Ubiquitin and the Proteasome. *Nat. Rev. Mol. Cell Biol.* **2005**, *6*, 79–87.

(2) Dalton, W. S. The proteasome. *Semin. Oncol.* **2004**, *31*, 3–9.

(3) Kisselev, A. F.; Goldberg, A. L. Proteasome inhibitors: from research tools to drug candidates. *Chem. Biol.* **2001**, *8*, 739–758.

(4) Adams, J. The proteasome: a suitable antineoplastic target. *Nat. Rev. Cancer* **2004**, *4*, 349–360.

(5) Goldberg, A. L. Functions of the proteasome: from protein degradation and immune surveillance to cancer therapy. *Biochem. Soc. Trans.* **2007**, *35*, 12–17.

(6) Groll, M.; Ditzel, L.; Löwe, J.; Stock, D.; Bochtler, M.; Bartunik, H. D.; Huber, R. Structure of 20S proteasome from yeast at 2.4 Å resolution. *Nature (London)* **1997**, *386*, 463–471.

(7) Orlowski, M.; Wilk, S. Catalytic activities of the 20S proteasome, a multicatalytic proteinase complex. *Arch. Biochem. Biophys.* **2000**, *383*, 1–16.

(8) Kisselev, A. F.; Callard, A.; Goldberg, A. L. Importance of the different proteolytic sites of the proteasome and the efficacy of inhibitors varies with the protein substrate. *J. Biol. Chem.* **2006**, *281*, 8582–8590.

(9) Groll, M.; Heinemeyer, W.; Jäger, S.; Ullrich, T.; Bochtler, M.; Wolf, D. H.; Huber, R. The catalytic sites of 20S proteasomes and their role in subunit maturation: a mutational and crystallographic study. *Proc. Natl. Acad. Sci. U.S.A.* **1999**, *96*, 10976–10983.

(10) Rock, K. L.; Gramm, C.; Rothstein, L.; Clark, K.; Stein, R.; Dick, L.; Hwang, D.; Goldberg, A. L. Inhibitors of the proteasome block the degradation of most cell proteins and the generation of peptides presented on MHC class I molecules. *Cell* **1994**, *78*, 761–771.

(11) Rock, K. L.; York, I. A.; Saric, T.; Goldberg, A. L. Protein degradation and the generation of MHC class I presented peptides. *Adv. Immunol.* **2002**, *80*, 1–70.

(12) Rivett, A. J.; Hearn, A. R. Proteasome function in antigen presentation: immunoproteasome complexes, peptide production, and interactions with viral proteins. *Curr. Protein Pept. Sci.* **2004**, *5*, 153–161.

(13) Adams, J.; Behnke, M.; Chen, S.; Cruickshank, A. A.; Dick, L. R.; Grenier, L.; Klunder, J. M.; Ma, Y. T.; Plamondon, L.; Stein, R. L. Potent and selective inhibitors of the proteasome: dipeptidyl boronic acids. *Bioorg. Med. Chem. Lett.* **1998**, *8*, 333–338.

(14) Orlowski, R. Z.; Stinchcombe, T. E.; Mitchell, B. S.; Shea, T. C.; Baldwin, A. S.; Stahl, S.; Adams, J.; Esseltine, D. L.; Elliott, P. J.; Pien, C. S.; Guerciolini, R.; Anderson, J. K.; Depcik-Smith, N. D.; Bhagat, R.; Lehman, M. J.; Novick, S. C.; O'Connor, O. A.; Soignet, S. L. Phase I trial of the proteasome inhibitor PS-341 in patients with refractory hematologic malignancies. *J. Clin. Oncol.* **2002**, *20*, 4420–4427.

(15) Richardson, P. G.; Barlogie, B.; Berenson, J.; Singhal, S.; Jagannath, S.; Irwin, D.; Rajkumar, S. V.; Srkalovic, G.; Alsina, M.; Alexanian, R.; Siegel, D.; Orlowski, R. Z.; Kuter, D.; Limentani, S. A.; Lee, S.; Hideshima, T.; Esseltine, D. L.; Kauffman, M.; Adams, J.; Schenkein, D. P.; Anderson, K. C. A phase 2 study of bortezomib in relapsed, refractory myeloma. *N. Engl. J. Med.* **2003**, *348*, 2609–2617.

(16) Richardson, P. G.; Sonneveld, P.; Schuster, M. W.; Irwin, D.; Stadtmauer, E. A.; Facon, T.; Harousseau, J. L.; Ben-Yehuda, D.; Lonial, S.; Goldschmidt, H.; Reece, D.; San-Miguel, J. F.; Bladé, J.; Boccadoro, M.; Cavenagh, J.; Dalton, W. S.; Boral, A. L.; Esseltine, D. L.; Porter, J. B.; Schenkein, D.; Anderson, K. C. Bortezomib or high-dose dexamethasone for relapsed multiple myeloma. *N. Engl. J. Med.* **2005**, *352*, 2487–2498.

(17) Orlowski, R. Z.; Nagler, A.; Sonneveld, P.; Bladé, J.; Hajek, R.; Spencer, A.; San Miguel, J.; Robak, T.; Dmoszynska, A.; Horvath, N.; Spicka, I.; Sutherland, H. J.; Suvorov, A. N.; Zhuang, S. H.; Parekh, T.; Xiu, L.; Yuan, Z.; Rackoff, W.; Harousseau, J. L. Randomized phase III study of pegylated liposomal doxorubicin plus bortezomib compared with bortezomib alone in relapsed or refractory multiple myeloma: combination therapy improves time to progression. *J. Clin. Oncol.* **2007**, *25*, 3892–3901.

(18) O'Connor, O. A.; Wright, J.; Moskowitz, C.; Muzzy, J.; MacGregor-Cortelli, B.; Stubblefield, M.; Straus, D.; Portlock, C.; Hamlin, P.; Choi, E.; Dumetrescu, O.; Esseltine, D.; Trehu, E.; Adams, J.; Schenkein, D.; Zelenetz, A. D. Phase II clinical experience with the novel proteasome inhibitor bortezomib in patients with indolent non-Hodgkin's lymphoma and mantle cell lymphoma. *J. Clin. Oncol.* **2005**, *23*, 676–684.

(19) Goy, A.; Younes, A.; McLaughlin, P.; Pro, B.; Romaguera, J. E.; Hagemeister, F.; Fayad, L.; Dang, N. H.; Samaniego, F.; Wang, M.; Broglio, K.; Samuels, B.; Gilles, F.; Sarris, A. H.; Hart, S.; Trehu, E.; Schenkein, D.; Cabanillas, F.; Rodriguez, A. M. Phase II study of proteasome inhibitor bortezomib in relapsed or refractory B-cell non-Hodgkin's lymphoma. *J. Clin. Oncol.* **2005**, *23*, 667–675.

(20) Richardson, P. G.; Briemberg, H.; Jagannath, S.; Wen, P. Y.; Barlogie, B.; Berenson, J.; Singhal, S.; Siegel, D. S.; Irwin, D.; Schuster, M.; Srkalovic, G.; Alexanian, R.; Rajkumar, S. V.; Limentani, S.; Alsina, M.; Orlowski, R. Z.; Najarian, K.; Esseltine, D.; Anderson, K. C.; Amato, A. A. Frequency, characteristics and reversibility of peripheral neuropathy during treatment of advanced multiple myeloma with bortezomib. *J. Clin. Oncol.* **2006**, *24*, 3113–3120.

(21) Lonial, S.; Waller, E. K.; Richardson, P. G.; Jagannath, S.; Orlowski, R. Z.; Giver, C. R.; Jaye, D. L.; Francis, D.; Giusti, S.; Torre, C.; Barlogie, B.; Berenson, J. R.; Singhal, S.; Schenkein, D. P.; Esseltine, D. L.; Anderson, J.; Xiao, H.; Heffner, L. T.; Anderson, K. C. Risk factors and kinetics of thrombocytopenia associated with bortezomib for relapsed, refractory multiple myeloma. *Blood* **2005**, *106*, 3777–3784.

(22) Demo, S. D.; Kirk, C. J.; Aujay, M. A.; Buchholz, T. J.; Dajee, M.; Ho, M. N.; Jiang, J.; Laidig, G. J.; Lewis, E. R.; Parlati, F.; Shenk, K. D.; Smyth, M. S.; Sun, C. M.; Vallone, M. K.; Woo, T. M.; Molineaux, C. J.; Bennett, M. K. Antitumor activity of PR-171, a novel irreversible inhibitor of the proteasome. *Cancer Res.* **2007**, *67*, 6383–6391.

(23) Bennett, M. K.; Kirk, C. J. Development of proteasome inhibitors in oncology and autoimmune diseases. *Curr. Opin. Drug Discovery Dev.* **2008**, *11*, 616–625.

(24) Groll, M.; Kim, K. B.; Kairies, N.; Huber, R.; Crews, C. M. Crystal structure of epoxomicin: 20S proteasome reveals a molecular basis for selectivity of β-epoxyketone proteasome inhibitors. *J. Am. Chem. Soc.* **2000**, *122*, 1237–1238.

(25) Hanada, M.; Sugawara, K.; Kaneta, K.; Toda, S.; Nishiyama, Y.; Tomita, K.; Yamamoto, H.; Konishi, M.; Oki, T. Epoxomicin, a new antitumor agent of microbial origin. *J. Antibiot. (Tokyo)* **1992**, *45*, 1746–1752.

(26) Sin, N.; Kim, K. B.; Elofsson, M.; Meng, L.; Auth, H.; Kwok, B. H.; Crews, C. W. Total synthesis of the potent proteasome inhibitor epoxomicin: a useful tool for understanding proteasome biology. *Bioorg. Med. Chem. Lett.* **1999**, *9*, 2283–2288.

(27) Meng, L.; Mohan, R.; Kwok, B.; Sin, N.; Crews, C. M. Eponemycin exerts its antitumor effect through the inhibition of proteasome function. *Cancer Res.* **1999**, *59*, 2798–2801.

(28) Meng, L.; Mohan, R.; Kwok, B.; Elofsson, M.; Sin, N.; Crews, C. M. Epoxomicin, a potent and selective proteasome inhibitor, exhibits in vivo anti-inflammatory activity. *Proc. Natl. Acad. Sci. U.S.A.* **1999**, *96*, 10403–10408.

(29) Kuhn, D. J.; Chen, Q.; Voorhees, P. M.; Strader, J. S.; Shenk, K. D.; Sun, C. M.; Demo, S. D.; Bennett, M. K.; van Leeuwen, F. W.; Chanan-Khan, A. A.; Orlowski, R. Z. Potent activity of carfilzomib, a novel, irreversible inhibitor of the ubiquitin−proteasome pathway, against preclinical models of multiple myeloma. *Blood* **2007**, *110*, 3281–3290.

(30) O'Connor, O. A.; Orlowski, R. Z.; Alsina, M.; Stewart, K.; Trudel, S.; Vallone, M. K.; Woo, T. M.; Urquilla, P. R.; Molineaux, C. J.; Goy, A. Multicenter phase I studies to evaluate the safety, tolerability, and clinical response to intensive dosing with the proteasome inhibitor PR-171 in patients with relapsed or refractory hematological malignancies [abstract]. *Blood (ASH Annual Meeting Abstracts)* **2006**, *108*, 2430.

(31) Stapnes, C.; Døskeland, A. P.; Hatfield, K.; Ersvaer, E.; Ryningen, A.; Lorens, J. B.; Gjertsen, B. T.; Bruserud, O. The proteasome inhibitors bortezomib and PR-171 have antiproliferative and proapoptotic effects on primary human acute myeloid leukaemia cells. *Br. J. Hamaetol.* **2007**, *136*, 814–828.

(32) Orlowski, R. Z.; Stewart, K.; Vallone, M.; Molineaux, C.; Kunkel, L.; Gericitano, J.; O'Connor, O. A. Safety and antitumor efficacy of the proteasome inhibitor carfilzomib (PR-171) dosed for five consecutive days in hematologic malignancies: Phase I results. *Blood* **2007**, *110*, 409.

(33) Alsina, M.; Trudel, S.; Vallone, M.; Molineaux, C.; Kunkel, L.; Goy, A. Phase I single agent antitumor activity of twice weekly consecutive day dosing of the proteasome inhibitor carfilzomib (PR-171) in hematologic malignancies. *Blood* **2007**, *110*, 411.

(34) Demo, S. D.; Kirk, C., J.; Parlati, F.; Aujay, M. A. et al. A proteasome active site ELISA (PASE) for rapid quantitation of proteasome activity in vitro and in vivo. Manuscript in preparation.

(35) Harker, W. G.; MacKintosh, F. R.; Sikic, B. I. Development and characterization of a human sarcoma cell line, MES-SA, sensitive to multiple drugs. *Cancer Res.* **1983**, *43*, 4943–4950.

(36) Obach, R. S. Predication of human clearance of twenty-nine drugs from hepatic microsomal intrinsic clearance data: An examination of in vitro half-life approach and nonspecific binding to microsomes. *Drug Metab. Dispos.* **1999**, *27*, 1350–1359.

(37) Pauletti, G. M. Peptidomimetics designed for oral absorption. *Adv. Amino Acid Mimetics Peptidomimetics* **1999**, *2*, 89–123.

(38) Hamman, J. H.; Enslin, G. M.; Kotzé, A. F. Oral delivery of peptide drugs. *Biodrugs* **2005**, *19*, 165–177.

(39) Vinitsky, A.; Cardozo, C.; Sepp-Lorenzino, L.; Michaud, C.; Orlowski, M. Inhibition of the proteolytic activity of the multicatalytic proteinase complex (proteasome) by substrate-related peptidyl aldehydes. *J. Biol. Chem.* **1994**, *269*, 29860–29866.

(40) Shenk, K. D.; Parlati, F.; Zhou, H. J.; Sylvain, C.; Smyth, M. S.; Bennett, M. K.; Laidig, G. J. Preparation of peptide epoxyketones as selective immunoproteasome inhibitors. U.S. Patent 2007293465 A1 20071220, 2007.

(41) Fretland, A. J.; Omiecinski, C. J. Epoxide hydrolases: biochemistry and molecular biology. *Chem.-Biol. Interact.* **2000**, *129*, 41–59.

(42) Laidig, G. J.; Radel, P. A.; Smyth, M. S. Synthesis of amino acid keto-epoxide. U.S. Patent 2005256324 A1 20051117, 2005.

(43) Zhou, H. J.; Sun, C. M.; Shenk, K. D.; Laidig, G. J. Compounds for enzyme inhibition. U.S. Patent 2007105786 A1 20070510, 2007.

(44) Kim, S.; Lee, J. I.; Kim, Y. C. A simple and mild esterification method for carboxylic acids using mixed carboxylic−carbonic anhydrides. *J. Org. Chem.* **1985**, *50*, 560–565.

JM801329V